Plasma Analysis
Application Note 231

EQP

An Improved Method for the Study of Neutral Components of Processing Plasma

Summary

For a number of applications of electrical plasmas in surface processing it is helpful to know the nature and relative abundances of the neutral species present in the plasma, both long and short-lived species. This is the case, for example, in the plasma-enhanced deposition of diamond films using hydrogen/methane plasmas.

In the past, various research groups have studied such plasmas by sampling neutral species, including radicals, from the plasma and examining the ionisation efficiency of the various species as a function of the plasma conditions, using the Hiden EQP instrument.

The present note discusses the potential advantages of examining the neutral components through the efficiency with which they form negative ions by electron attachment, rather than positive ions by electron impact ionisation.

Manufactured in England by:

HIDEN ANALYTICAL LTD
420 Europa Boulevard, Warrington, WA5 7UN, England
t: +44 (0) 1925 445225 f: +44 (0) 1925 416518
e: info@hiden.co.uk w: www.HidenAnalytical.com

Basic Principles

Many of the gases used in plasma processing are electronegative (for example: fluorocarbons, methane, sulphur hexafluoride, silane) and the negative ions formed in the plasmas are important for the control of the deposition or etching processes concerned. The neutral fragments produced in the plasmas are of equal or greater importance. Fortunately, many of these fragments are themselves species which form negative ions, when bombarded with electrons, by mechanisms such as associative or dissociative attachment or pair-production. The probabilities of forming negative ions through reactions such as

$$e + x \rightarrow x^-$$

or $$e + xy \rightarrow x^- + y$$

or $$e + xy \rightarrow x^- + y^+ + e$$

are well-known for many species and available as values of the so-called "attachment cross-section" as a function of the electron energy.

For the present application, it is an attractive feature of many of the attachment cross-section curves (see figure 1 for carbon dioxide, for example) that a well-defined peak occurs at low energies. This behaviour may be contrasted with that for the corresponding ionisation cross-section which generally increases smoothly with electron energy above some threshold value and reaches a broad maximum at around 70eV. Typical attachment cross-sections for species known to be of interest in plasma processing are shown in figure 2. The data show clearly the significant differences between the curves for the various species.

It is possible, using the EQP system, to measure attachment cross-sections such as those shown in figures 1 and 2 for neutral species sampled from a plasma.

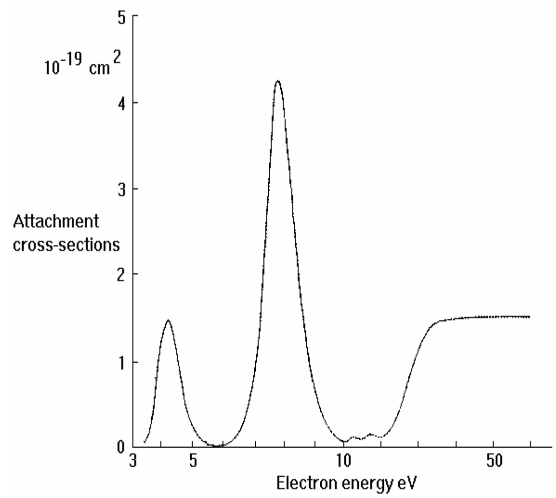

Figure 1

Experimental Data

a) Attachment cross sections

To illustrate the capability of the EQP to generate data such as that of figures 1 and 2, experiments were carried out using a plasma generated in carbon dioxide.

Measurements were first taken without the plasma being turned on. The cross-section curve measured was as shown in figure 3. With the plasma operating, the measured cross-sections were as shown in figure 4. It is clear that the peak at around 8eV in figure 3 has been joined in figure 4 by an additional peak at around 10eV.

The data in figures 3 and 4 were obtained with the mass spectrometer set to detect O^- ions, i.e. figure 3 refers to the process

$e + CO_2 \rightarrow O^- +$ other fragments

which is known to have a maximum probability for an electron energy of 8.3eV. The simplest explanation of the extra peak at 10eV in figure 4 is that it refers to the process

$e + CO \rightarrow O- + C$

which is known to peak at 10.1eV. The carbon monoxide is assumed to have been produced in the plasma by dissociation of the carbon dioxide.

To confirm this hypothesis, the carbon dioxide in the plasma cell was replaced by carbon monoxide and with the plasma off, the data of figure 5 were obtained. The main peak at 10eV is clearly visible and there are residual peaks at 4 and 8eV due to the fact that not all the carbon dioxide from the previous experiment had been removed from the system.

b) Ion energy distributions

It is known that the kinetic energies of the negative ions formed by electron attachment are a function of the electron energy. Figure 6 shows, for example, the variation of the mean energy of Cl^- ions formed by the reaction

$$e + SO_2Cl_2 \rightarrow Cl^- + Cl + SO_2$$

as a function of the electron energy. (The figure also shows the attachment cross-section curve).

The present experiments confirmed a dependence of the energy of the ions on that of the electrons. Figure 7 shows typical data for the O^- ions produced at electron energies of 70eV, 8.5eV and 4.2eV. The ion energy distribution at an electron energy of 4.2eV is of particular interest. It should be noted that the ion energy scale of figure 7 is an arbitrary one. The data of figure 4 were obtained at an ion energy corresponding to that of the peak ion current of figure 7.

Applications

There are clearly a number of ways in which data such as those of figures 4 - 7 could be utilised. For example, the presence of electronegative neutral molecules/radicals in a processing plasma can be readily detected and the relative abundances of various neutral species can be determined, as a function of the plasma conditions, and can be used to optimise the conditions for a particular process.

The time history of a particular process can also be followed through the monitoring of one or more electronegative species produced in the plasma. There is a possibility that end point detection may be simplified if a given neutral species is a particularly sensitive component of the plasma.

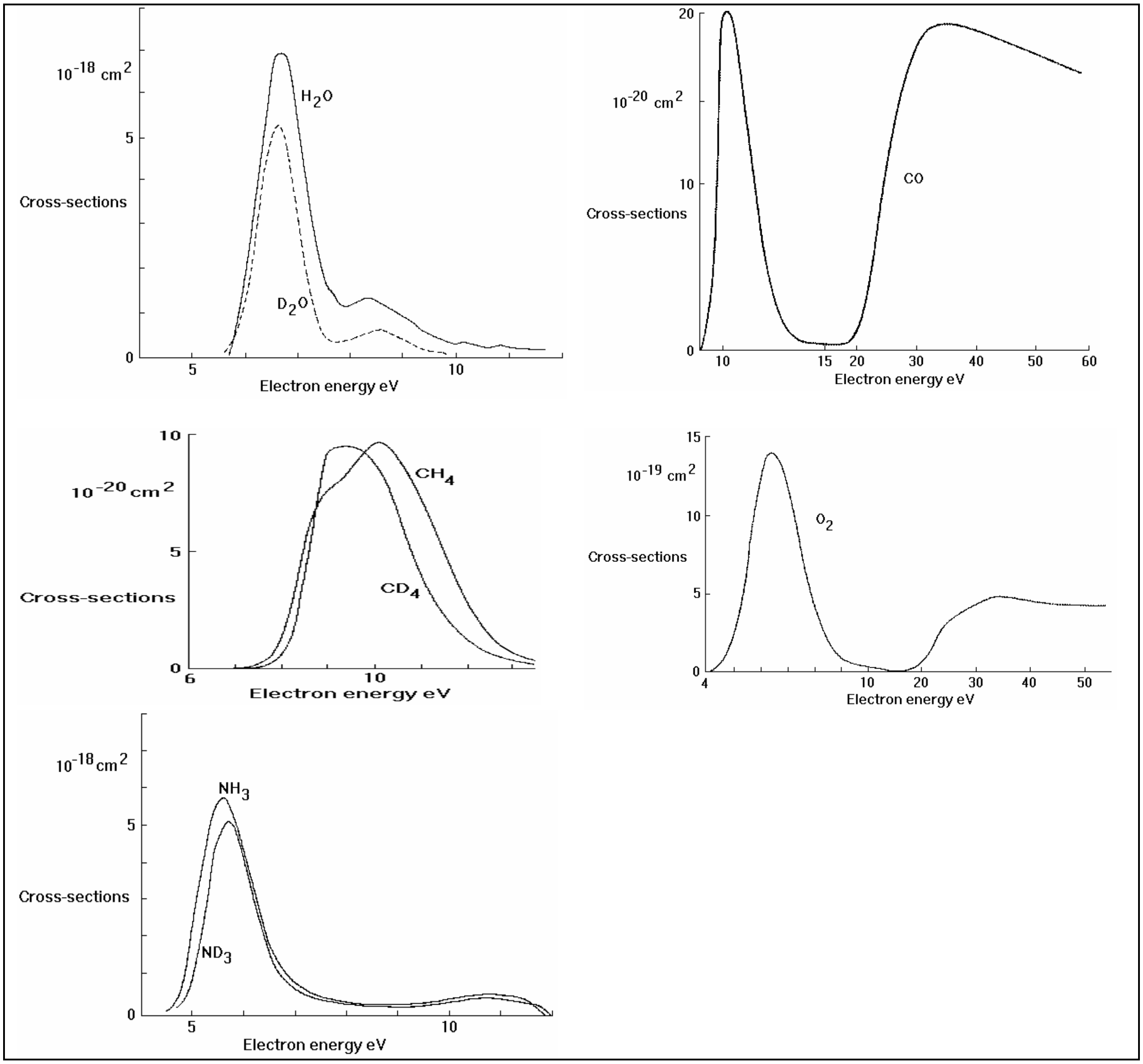

10^{-18} cm^2
Cross-sections
H$_2$O
D$_2$O
Electron energy eV
10^{-20} cm^2
Cross-sections
CO
Electron energy eV
10^{-20} cm^2
Cross-sections
CH$_4$
CD$_4$
Electron energy eV
10^{-19} cm^2
Cross-sections
O$_2$
Electron energy eV
10^{-18} cm^2
Cross-sections
NH$_3$
ND$_3$
Electron energy eV

Figure 2

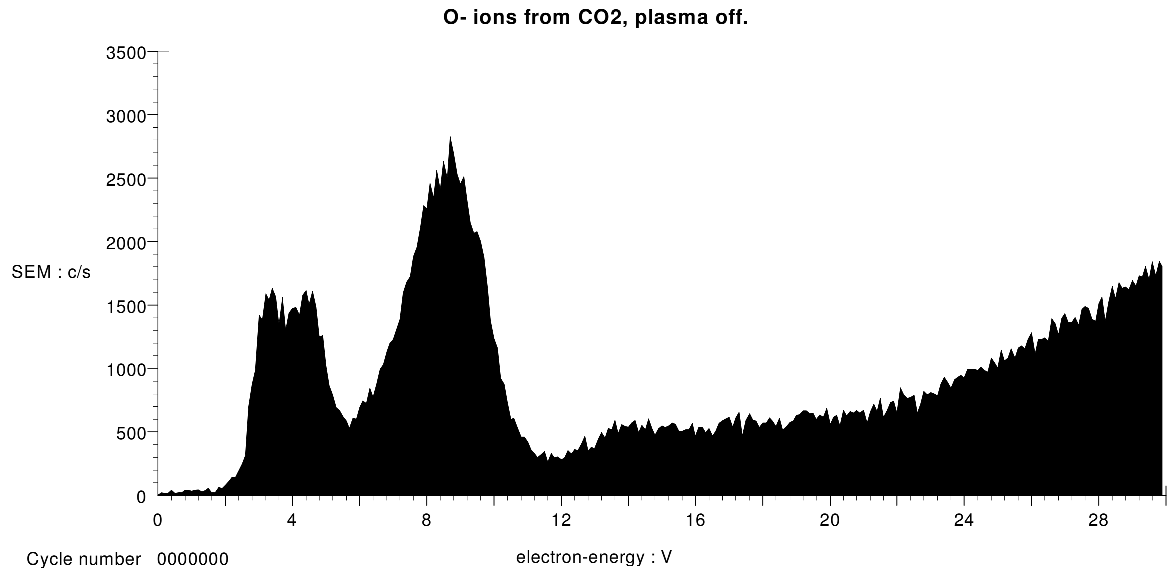

Figure 3

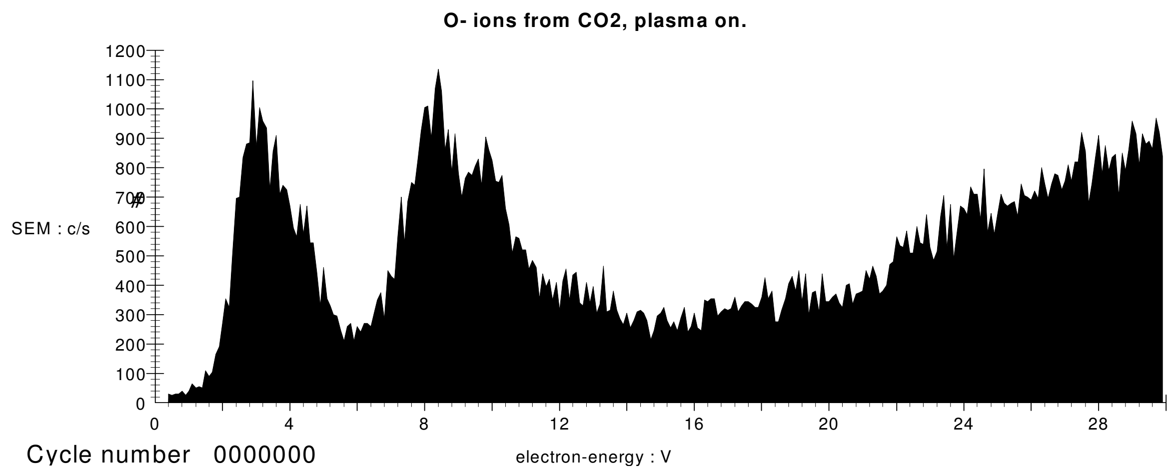

Figure 4

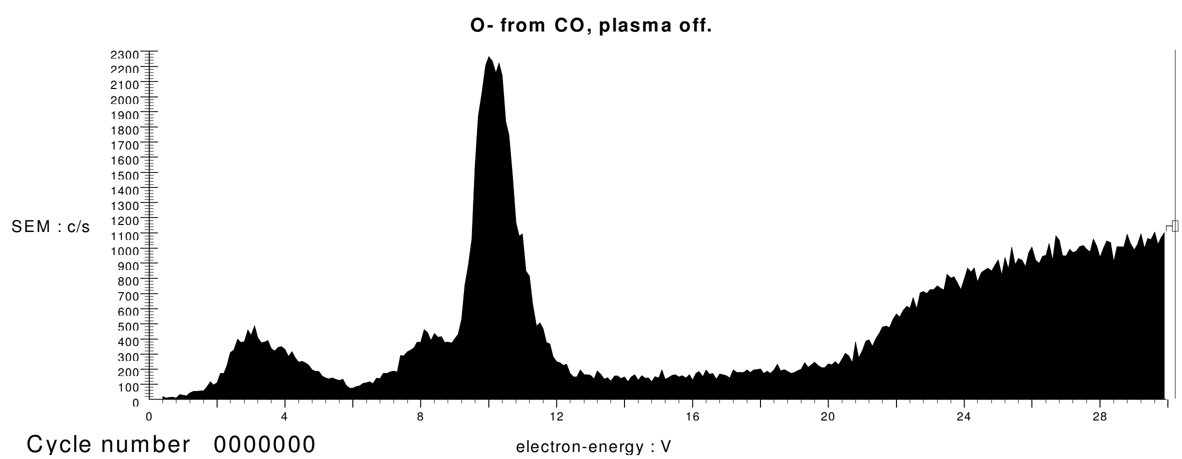

Figure 5

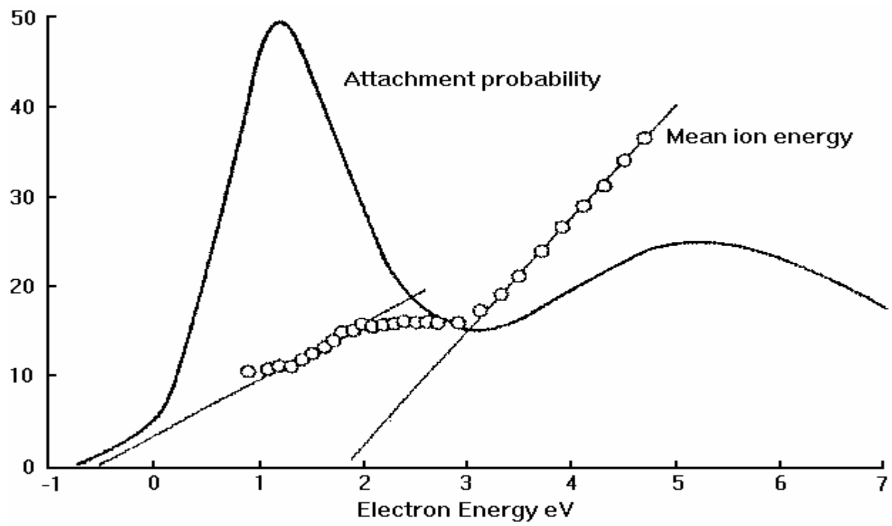

Figure 6

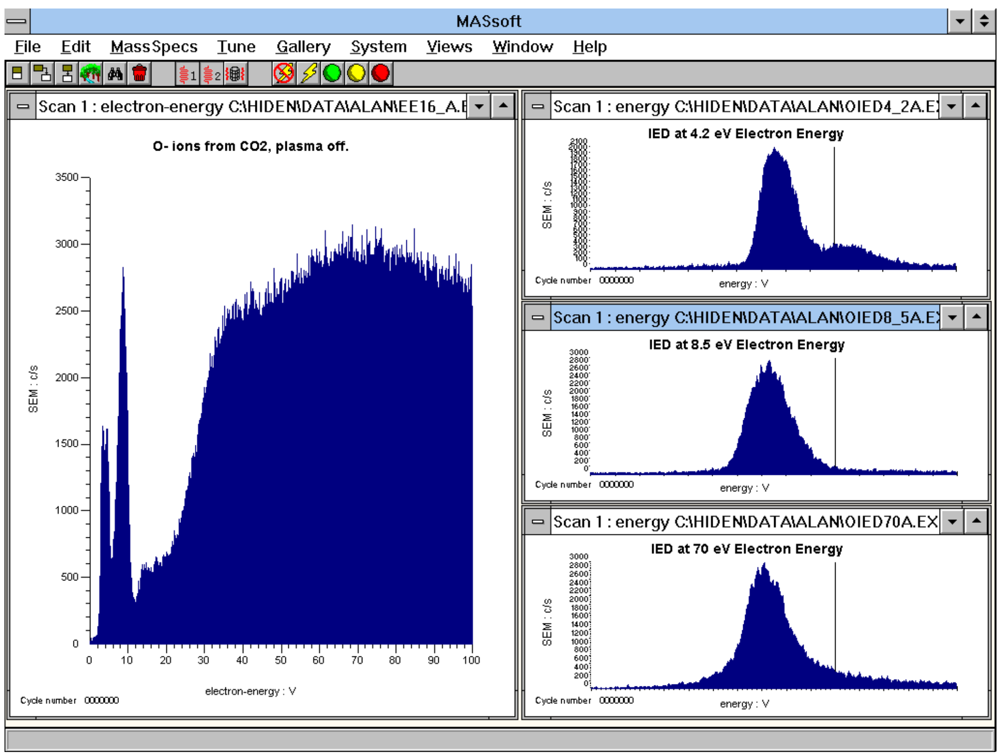

Figure 7